

Ab initio band-structure calculations for alkaline-earth oxides and sulfides

Ravindra Pandey, J. E. Jaffe, and A. Barry Kunz

Department of Physics, Michigan Technological University, Houghton, Michigan 49931

(Received 28 September 1990)

The electronic structure of the oxides and sulfides of Mg, Ca, and Sr is computed with use of the self-consistent Hartree-Fock method including correlation. Energy-band structure and density of states are presented and discussed in context with the available experimental and theoretical studies. Our results predict that these materials (except MgS) are direct-band-gap materials.

I. INTRODUCTION

Alkaline-earth oxides are technologically important materials with applications ranging from catalysis to microelectronics. Alkaline-earth sulfides have been proposed as host materials for device applications such as multicolor thin-film electroluminescent and magneto-optical devices.¹

Recently, Kaneko and his co-workers² have measured the optical spectrum of Ca, Sr, and Ba chalcogenides. They have interpreted their results on the basis of a self-consistent augmented-plane-wave (APW) band-structure calculation concluding that these materials, except BaO, are indirect-band-gap materials with the lowest direct band gap at the X point. However, a more detailed look at the experimental results and their interpretation reveals some inconsistencies.

(i) The appearance of the two groups of peaks (assigned to the excitons at the X point and Γ point, respectively) in the [imaginary part of $\epsilon(\omega)$] ϵ_2 spectrum showed no systematic trend in the oxides. It was absent in CaO and BaO, but was present in SrO.

(ii) It appears that the direct band gap in these materials was estimated from the ϵ_2 spectrum without taking account of the excitonic binding energy. [see Tables I and II of Ref. 2(a)].

(iii) None of the peaks in the ϵ_2 spectrum of CaO was assigned to the $\Gamma_{15}-\Gamma_1$ transition, but the assignment for the higher-order transition $\Gamma_{15}-\Gamma'_{25}$ and $\Gamma_{15}-\Gamma_{12}$ was given.

It is well known that band-structure calculations based on the local-density approximation (LDA) underestimate both the band gap and the valence-band width. Furthermore, the drastic lowering of the d -like conduction level (relative to the experiment) at the X point (i.e., X_3) has been observed in the LDA results for ionic materials such as NaCl.³ Hence we believe that the reported interpretation of the optical spectrum has not properly taken account of the inherent limitations of the LDA-based calculations and is therefore somewhat ambiguous.

To provide a more accurate basis for the interpretation of the optical spectrum of these materials, we have undertaken a detailed and systematic investigation of the electronic structure of alkaline-earth chalcogenides using the Hartree-Fock method. This method has been highly suc-

cessful in describing the electronic structure of alkali and silver halides.³ The present work focuses on the nature of the energy gap of the oxides and sulfides of Mg, Ca, and Sr only. In the next section, we give a detailed account of the Hartree-Fock method including electron-correlation effects. In Sec. III the results are presented and compared to earlier studies involving both theory and experiment. Finally, conclusions are given in Sec. IV.

II. THEORETICAL METHOD

The basic method is Hartree-Fock and we begin with the canonical Fock equation,

$$F\phi_i(\mathbf{k}, \mathbf{x}_i) = \epsilon_i(\mathbf{k})\phi_i(\mathbf{k}, \mathbf{x}_i), \quad (2.1)$$

where the one-electron orbitals, ϕ 's, are constrained to be orthonormal and eigenstates of the z component of spin and all pertinent crystal-symmetry operations. The Fock operator F is given by

$$F = \frac{-\hbar^2}{2m}\nabla^2 - \sum_I \frac{Z_I e^2}{|\mathbf{r} - \mathbf{R}_I|} + e^2 \int \frac{\rho(\mathbf{x}', \mathbf{x}')}{|\mathbf{r} - \mathbf{r}'|} d\mathbf{x}' - e^2 \int \frac{\rho(\mathbf{x}, \mathbf{x}')}{|\mathbf{r} - \mathbf{r}'|} P(\mathbf{x}', \mathbf{x}) d\mathbf{x}, \quad (2.2)$$

We note here that the Fock operator is a unique functional of the first-order density matrix ρ , which is given by

$$\rho(\mathbf{x}, \mathbf{x}') = \sum_{\mathbf{k}} \sum_i \phi_i^*(\mathbf{k}, \mathbf{x}) \phi_i(\mathbf{k}, \mathbf{x}'), \quad (2.3)$$

where the sum is carried over all occupied orbitals.

For the N -electron-system ground state, the occupied one-electron orbitals, ϕ 's are the ones with the N lowest values of the Fock eigenvalue $\epsilon_i(\mathbf{k})$. In the context of Koopmans's theorem, the eigenvalue of an occupied orbital $\epsilon_i(\mathbf{k})$ is the negative of the energy needed to remove the electron (occupying the i th orbital) from the crystal, and the eigenvalue $\epsilon_a(\mathbf{k})$ for a virtual (unoccupied) orbitals is the negative of the energy gained by adding an electron to the crystal. In both cases, the electronic density of the remaining electrons is unrelaxed. Hence the physics here refers to ionization properties, not to excitation properties of the N -electron system.

The self-consistent solution of the Fock equation (2.1)

is a cumbersome process for a crystal, and the iterative nature of the procedure demands that this equation be solved several times, making it a time-consuming operation. One may therefore construct a three-dimensional mesh in \mathbf{k} space and then solve the Fock equation for a few \mathbf{k} points, obtaining the density matrix ρ for the crystal. Alternatively one may use a method proposed by Kunz³ to obtain a self-consistent density matrix. Kunz's method is based on the local-orbital theory of Adams and Gilbert,⁴ solving the modified Fock equation

$$(F + \rho W \rho) \hat{\phi}_i(\mathbf{r} - \mathbf{R}_A) = \varepsilon_i \hat{\phi}_i(\mathbf{r} - \mathbf{R}_A), \quad (2.4)$$

and requiring that the occupied orbitals $\hat{\phi}_i$'s (which are a set of atomiclike orbitals centered on \mathbf{R}_A) be obtainable from linear transformations of occupied (canonical) Fock orbitals ϕ_j 's. The density matrix remains invariant and is now given by

$$\rho = \sum_{\substack{A_i, \\ B_j}} \hat{\phi}_i(\mathbf{x} - \mathbf{R}_A) S_{A_i B_j}^{-1} \hat{\phi}_j^*(\mathbf{x}' - \mathbf{R}_B) \quad (2.5)$$

and

$$S_{A_i B_j} = \int \hat{\phi}_i^*(\mathbf{x} - \mathbf{R}_A) \phi_j(\mathbf{x} - \mathbf{R}_B) d\mathbf{x}. \quad (2.6)$$

Thus solving Eq. (2.4) provides the ρ needed to obtain the Fock operator F for any choice of the operator W . Ideally, one picks a set of W 's to produce localized atomiclike, orbital solutions. (This can be accomplished by requiring W 's to be a potential well centered on a site representing the crystalline environment most efficiently.)

If we wish to localize N_A electrons on each site A in the crystal, then we solve the Eq. (2.4) for each site in the crystal using the first N_A solutions from each equation to build up a set of local orbitals, $\hat{\phi}_i(\mathbf{x} - \mathbf{R}_A)$, which exactly span the occupied part of the Fock space. Crystal symmetry then allows that we must solve only m local orbital equations for a crystal with m atoms in the unit cell. That is, in terms of the local orbitals, the occupied Fock space is exactly determined by a minimum basis set. Finally, we construct the Fock operator using the first-order density matrix ρ and solve the equation (2.1), not iteratively, but once.

A Fock occupied orbital $\phi_j(\mathbf{k}, \mathbf{x})$ can be given as

$$\phi_j(\mathbf{k}, \mathbf{x}) = N^{-1/2} \sum_{l=\text{occ}} \sum_A a_l^j(\mathbf{k}) e^{i\mathbf{k} \cdot \mathbf{R}_A} \phi_l(\mathbf{x} - \mathbf{R}_A), \quad (2.7)$$

where the coefficients $a_l^j(\mathbf{k})$ are determined by diagonalizing the $m \times m$ matrix for the Fock operator in terms of the basis of Bloch projected local orbital solutions.

We note here that the expression for the first-order density matrix ρ involves elements of the inverse of the overlap matrix expressed by means of the Löwdin α -function expansion method

$$S_{A_i B_j}^{-1} = 2\delta_{A_i B_j} - S_{A_i B_j} + \dots, \quad (2.8)$$

which then allows everything to be expressed in terms of the overlap matrix itself.⁵ In this procedure, we keep terms which involve only first order in interatomic overlap. This is consistent with the assumption of a small

overlap between nearest neighbors for ionic crystals. That is, the assumption is made that the interatomic overlap between the local orbitals is small enough to allow accurate solutions to be obtained while retaining in the density matrix only terms which are of zero or first order in interatomic overlap.

Furthermore, we note here that the local-orbital solutions for the cation in the crystal typically differ by one part in 10^4 from free-ion solutions in terms of charge density. On the other hand, the anions in the crystal are found to be more localized than the same ion in free space. The anion crystal solutions differ by up to one part in 10^2 in terms of charge density from the free-ion solutions.

Since this procedure does not provide for the virtual (conduction) bands, we use the mixed-basis method (developed also by Kunz and his co-workers)³ consisting of a basis of all occupied orbitals [Eq. (2.7)] and a plane-wave set given by

$$\chi(\mathbf{k}, \mathbf{q}, \mathbf{r}) = (N\Omega)^{-1/2} \exp[i(\mathbf{k} + \mathbf{q}) \cdot \mathbf{r}], \quad (2.9)$$

where Ω is the unit-cell volume, \mathbf{k} is a vector in the first Brillouin zone, and \mathbf{q} is a reciprocal-lattice vector. For this study we use a set of 35 plane waves. We note here that in going from 15 to 27 plane waves, the conduction levels shift by about 0.3 eV over the first 20 eV, whereas in going from 27 to 59 plane waves, the shifts are 0.1 eV or less.

As is well known, Hartree-Fock energy bands for nonmetallic solids have exaggerated energy gaps. This is due to the fact that the single determinantal formulation in Hartree-Fock theory does not allow the electrons to interact in more than an average sense, and thus their motions are uncorrelated. Electrons of the same spin have some of their pair interaction taken into account due to the built-in antisymmetry of the wave function, but there is no pair correlation at all between electrons of opposite spin.

The correlation energy is conventionally defined as the difference between the energy obtained from the Hartree-Fock theory and the exact nonrelativistic energy of the system. In principle, the exact energy can be determined by using a wave function that is a linear combination of determinants. This technique is referred to as configuration interaction. However, we note here that the treatment of correlation effects in an infinite solid is not an easy and simple extension of the same in finite molecules. For solids, it is more practical to estimate the correlation correction by other methods.

We note here that the Hartree-Fock excitation energies are

$$\varepsilon_{n\mathbf{k}}^0 = E_{\text{HF}}^{(N)} - E_{\text{HG}}^{(N-1)} \quad (2.10a)$$

for occupied states and

$$\varepsilon_{n'\mathbf{k}'}^0 = E_{\text{HF}}^{(N+1)} - E_{\text{HF}}^{(N)} \quad (2.10b)$$

for unoccupied states. In going beyond the Hartree-Fock approximation, let us define the exact excitation energies as

$$\begin{aligned}\varepsilon_{nk} &= E^{(N)} - E^{(N-1)}, \\ \varepsilon_{n'k'} &= E^{(N+1)} - E^{(N)},\end{aligned}\quad (2.11)$$

where $E^{(N)}$ is the exact total energy of the N -electron system.

Assuming that the correlation effect can be treated by perturbation theory, we write

$$E^{(N)} = E_{\text{HF}}^{(N)} + E_c^{(N)}, \quad (2.12)$$

where $E_c^{(N)}$ is the correlation energy of the N -electron system. Equation (2.10) can now be written as

$$\begin{aligned}\varepsilon_{nk} &= E_{nk}^0 + (E_c^{(N)} - E_c^{(N-1)}), \\ \varepsilon_{n'k'} &= E_{n'k'}^0 + (E_c^{(N+1)} - E_c^{(N)}).\end{aligned}\quad (2.13)$$

For nonmetals in which the upper valence bandwidth is less than the Hartree-Fock band gap, Pantelides *et al.*⁶ have shown that Eq. (2.13) can be approximated by

$$\begin{aligned}\varepsilon_{nk} &= \varepsilon_{nk}^0 + E_{nk}^{(N-1)}(h), \\ \varepsilon_{n'k'}^{(N)} &= \varepsilon_{n'k'}^0 + E_{n'k'}^{(N)}(e).\end{aligned}\quad (2.14)$$

Here, $E_{n'k'}(e)$ is the self-energy of an electron that occupies the one-electron Hartree-Fock state $n'k'$ in an N -electron system. By analogy, $E_{nk}^{(N-1)}(h)$ is the total energy charge in the $(N-1)$ electrons when the electron occupying state nk is removed, and therefore it is referred to as the self-energy of a hole.

We use the electronic polaron model⁷ to calculate the self-energies of the electron and hole. In the Hartree-Fock theory, particles (i.e., conduction-band electrons and valence-band holes) respond only to the average position of the other electrons and nuclei. This is obviously incorrect since it is expected that the independent charge,

especially if it is moving slowly, will polarize its surroundings to some extent. The electronic polaron model dresses the conduction-band electrons and valence-band holes with quanta of the polarization-field excitons treating the energy bands as quasiparticle bands with the Hartree-Fock one-electron bands as a zeroth-order approximation to the quasiparticle bands.

In this model the excited states of a crystal are simulated by a dispersionless band of excitons so that $E^{(N)}(e)$ and $E^{(N-1)}(h)$ are the interaction energies of an electron and a hole with these excitons. The self-energies are then calculated by second-order perturbation theory.

The correction to the energy of an electron in a conduction band is given by

$$\Delta\varepsilon_e(k) = \frac{2\pi e^2 \hbar\omega_{ex}(1-1/\varepsilon_\infty)}{\Omega q^2} \sum_q \frac{|\langle k | e^{-iqr} | k-q \rangle|^2}{\varepsilon(k) - \hbar\omega_{ex} - \varepsilon(k-q)}, \quad (2.15)$$

where for a hole in a valence band

$$\begin{aligned}\Delta\varepsilon_h(k) &= \frac{2\pi e^2 \hbar\omega_{ex}(1-1/\varepsilon_\infty)}{\Omega q^2} \\ &\times \sum_q \frac{|\langle k | e^{-iqr} | k-q \rangle|^2}{\hbar\omega_{ex} + \varepsilon(k) - \varepsilon(k-q)}.\end{aligned}\quad (2.16)$$

Here $\hbar\omega_{ex}$ is the energy of the virtual polaron which we assume is constant and equal to the uncorrelated HF band gap, ε_∞ is the optical dielectric constant, and Ω is the unit-cell volume. The matrix element is taken between Bloch states of the band whose energy we are correcting (the uncorrected band energy appears in the denominators, and interband effects are ignored) and the sum runs over the first Brillouin zone. We perform the sum by sampling an irreducible wedge of the zone at 20

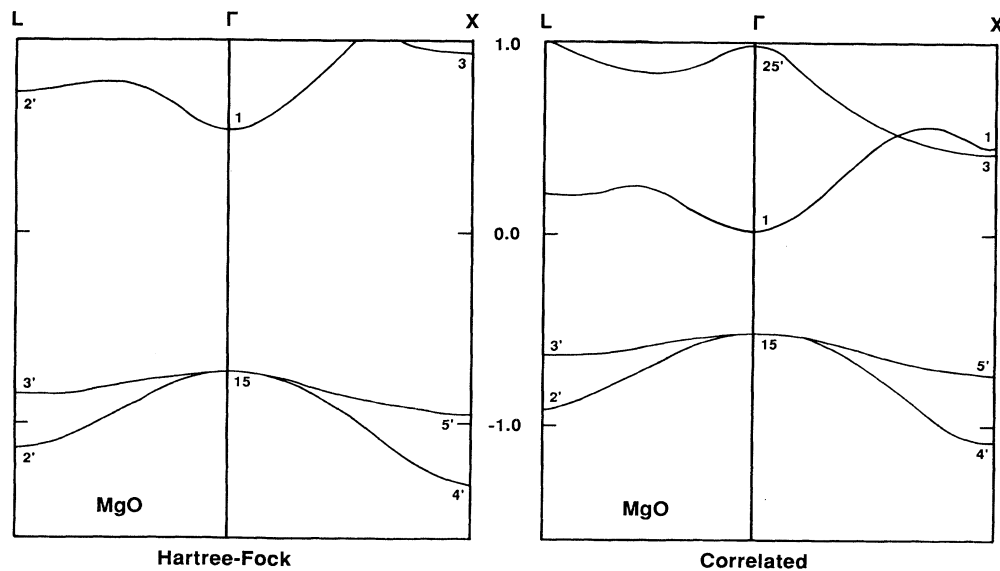


FIG. 1. MgO: Hartree-Fock and correlated energy bands.

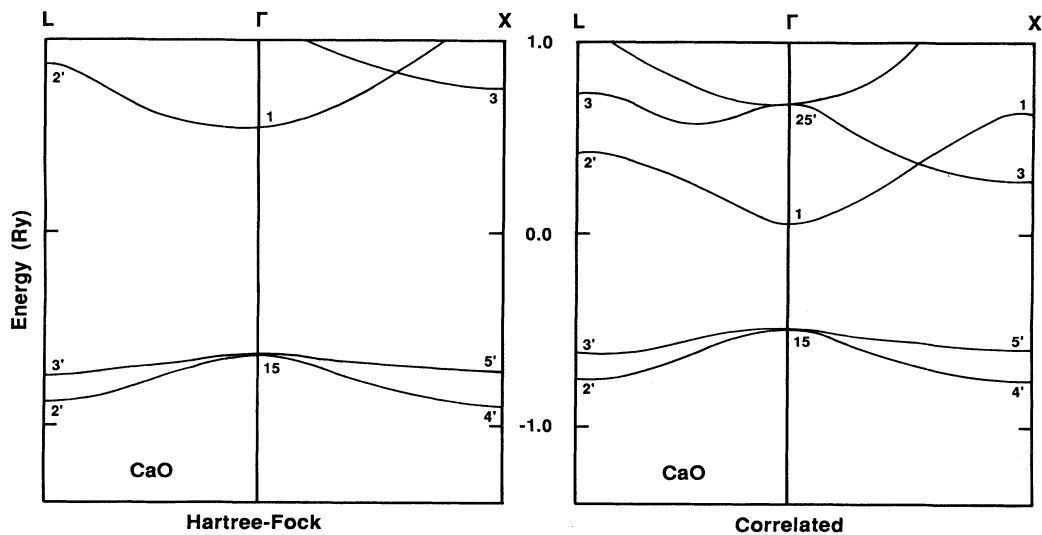


FIG. 2. CaO: Hartree-Fock and correlated energy bands.

points, with appropriate weight factors. The resulting corrections depend only slightly on the wave vector, so that they give nearly a rigid shift of the bands (downward for conduction bands and upward for valence bands). The positions of different valence bands relative to each other are also affected very little by this correction. By far the most noticeable effect of long-range correlation is the reduction of the band gap.

The electronic-polaron model neglects short-range correlation effects which are found to be important for insulators. Short-range correlation considers the relaxation of the nearby orbitals when an electron is added or removed. These corrections for the band in question are calculated by taking the difference between the binding

energy of the electron (obtained by an embedded-molecular-cluster calculation)⁸ and the equivalent Koopman's theorem binding energy (which is the energy of the level from which the electron is removed).

III. RESULTS AND DISCUSSION

A. Alkaline-earth oxides

The uncorrelated and correlated Hartree-Fock energy bands for MgO, CaO and SrO are shown in Figs. 1-3. The qualitative features in these band structures are found to be very similar to those in alkali halides. For example, anion p orbitals form the upper valence band.

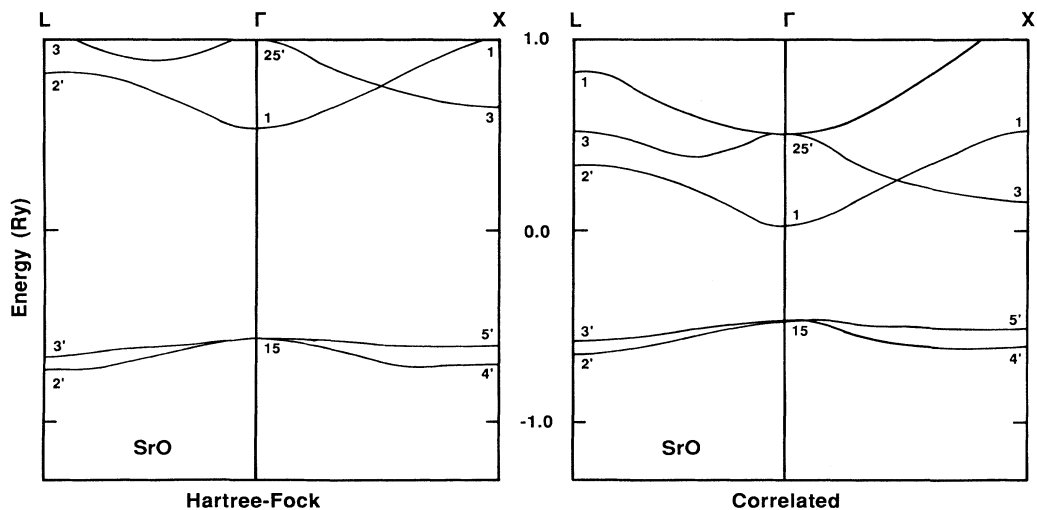


FIG. 3. SrO: Hartree-Fock and correlated energy bands.

TABLE I. Experimental energies for the major peaks in either optical absorption or the reflectivity spectrum of alkaline-earth oxides and sulfides.

		Peak energies (eV)
MgO	Reflectivity, ^a 80 K	7.7,10.8,13.2,16.8
CaO	Reflectivity, ^b 80 K	6.8,10,11.4,12.1,16.9
	Reflectivity, ^c 2 K	6.815
SrO	Absorption, ^d 300 K	5.77
	Reflectivity, ^c 2 K	5.727,5.79,6.05
CaS	Absorption, ^d 77 K	5.38
	Reflectivity, ^c 2 K	5.273,5.78
SrS	Absorption, ^d 77 K	4.8,4.9
	Reflectivity, ^c 2 K	4.761,4.855,5.321,5.425

^aRoessler and Walker, 1967 (Ref. 9).

^bWhited and Walker, 1969 (Ref. 10).

^cKaneko and Koda, 1988 (Ref. 2).

^dSaum and Hensley, 1959 (Ref. 11).

Both the valence-band maximum and the conduction-band minimum occur at the Γ point, predicting the oxides to be direct-band-gap materials.

Experimentally, the band gaps are usually estimated from optical spectra (either absorption or reflection). Table I displays such data on the oxides which have been used to estimate their band gap. (The band gap is taken to be the energy of the lowest-energy absorptivity or reflectivity peak plus the exciton binding energy.)

MgO is the simplest rocksalt-structure alkaline-earth chalcogenide, and a large number of both experimental and theoretical studies is therefore available to which we can compare our calculated results and subsequently judge the predictive capacity of the Hartree-Fock method used here. The present calculation predicts an uncorrelated band gap of 17.6 eV. When we include the correlation corrections (i.e., the long-range correction of 5.21 eV and the short-range correction of 4.9 eV), the band gap is reduced to 8.21 eV. The corresponding experimental value is 7.833 eV.¹² The energy gaps at high-symmetry points are given in Table II along with the results of the

earlier theoretical studies.¹³⁻²¹

The density of states for MgO is shown in Fig. 4. The upper valence band exhibits a double-peak character with a width of 7.64 eV. Recent photoemission data determines a width of 6.7 eV.¹⁵ The total valence-band width (i.e., *sp*-band width) comes out to be 24.9 eV as compared to the experimental value of about 21 eV.²² In Table III the calculated (electron) binding energies for core levels along with the corresponding *x*-ray photoelectron energies are given showing good agreement.

Several other theoretical studies on the band structure of MgO have been reported ranging from empirical pseudopotential to pseudofunction local-density approximation (LDA) (see Table II). Our calculation agrees with these studies in describing the qualitative features of the valence and conduction bands. Most of the calculations, including the present ones, agree in predicting that $E(\Gamma) < E(L) < E(X)$, where E is the energy gap. But these calculations differ considerably with each other in assigning the peaks in the ϵ_2 spectrum to different transitions. For example, Table IV lists the assignments of the

TABLE II. Energy gaps (in eV) at high-symmetry points for MgO.

Method	Γ	Direct gap	
		X	L
Experiment	7.833		
This work	8.21	15.79	11.48
APW-LDA ^a	4.98	9.62	9.31
Mixed basis (pseudopotential-LDA) ^b	4.36	11.0	8.0
Pseudofunction LDA ^c	4.63	11.0	9.8
Pseudopotential-LDA ^d	4.5	10.5	8.0
Tight-binding ^e	7.76	16.2	9.38
Hartree-Fock-LCAO ^f	8.9	16.9	11.7
Hartree-Fock-Slater ^g	7.53	19.05	11.50
KKR ^h	5.37		
Empirical pseudopotential ⁱ	7.78	12.35	10.89

^aStepanyuk *et al.*, 1989 (Ref. 13).

^bWang and Holzwarth, 1990 (Ref. 14).

^cBortz *et al.*, 1990 (Ref. 15).

^dChang and Cohen, 1984 (Ref. 16).

^eDaud, Jouanin, and Gout, 1977 (Ref. 17).

^fPantelides, Michish, and Kunz, 1977 (Ref. 18).

^gWalch and Ellis, 1973 (Ref. 19).

^hYamashita and Asano, 1970 (Ref. 20).

ⁱFong, Saslov, and Cohen, 1968 (Ref. 21).

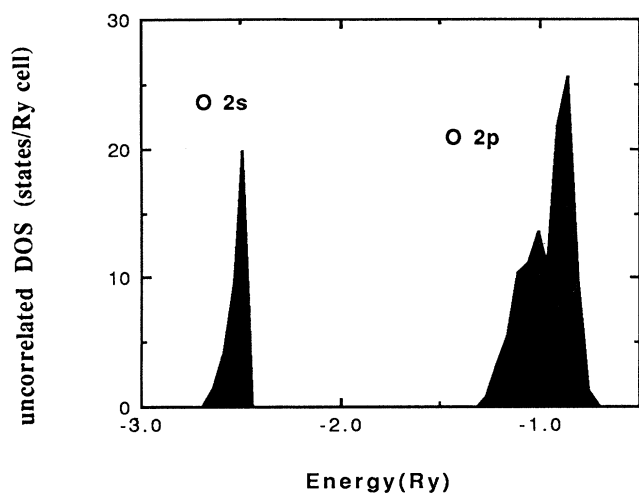


FIG. 4. MgO: density of states.

prominent peaks given by the three different approaches. Hence, it appears that a more detailed experimental study, such as angle-resolved photoemission spectroscopy (ARPES) method (which will not help if the disagreement comes from the conduction band), is required before anything can be said conclusively about the excitonic and/or interband transitions in MgO.

In CaO the uncorrelated band gap is predicted to be 15.9 eV. The inclusion of correlation correction (i.e., the long-range correction of 3.25 eV and the short-range correction of 4.9 eV) reduces the gap to 7.73 eV. The corresponding experimental value is 7.09 eV.¹² In Table V we list the energy gaps at high-symmetry points along with the results of other calculations based on augmented-plane-wave-linear combination of atomic orbitals (APW-LCAO),²⁵ tight-binding,²⁶ and combined tight-binding and pseudopotential¹⁷ methods.

The results for our calculation are in agreement with the earlier calculations for the valence-band configuration, predicting the valence-band maximum at Γ . However, the agreement disappears when we consider the conduction-band configuration. Our calculation, along with the tight-binding pseudopotential calculation, finds the conduction-band minimum at Γ , predicting that CaO is a direct-band-gap material. On the other hand, the APW-LCAO and tight-binding calculations deter-

TABLE III. Core binding energies of MgO, in eV.

	Core level ^a	This work	Expt.
Oxygen	2S (L_1)	23.8	22–23 ^b
	1S (K)	534.4	528.5 ^c
Magnesium	2p (L_{23})	47.6	46.2 ^b
	2S (L_1)	87.8	85.0 ^b
	1S (K)	1301.5	1299.8 ^c

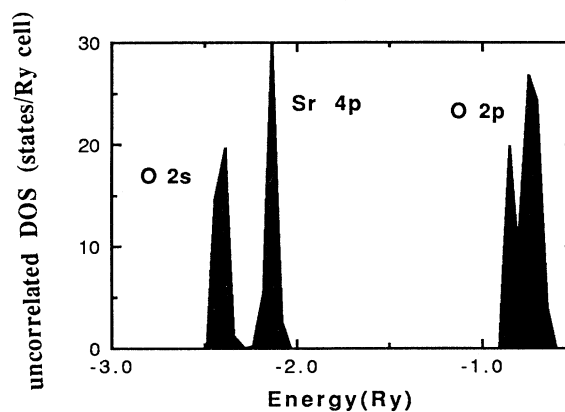
^aSpectroscopic notations are shown in the bracket.^bHanson, Arakawa, and Williams, 1972 (Ref. 23).^cFomichey, Zimkina, and Zhukova, 1969 (Ref. 24).

FIG. 5. SrO: density of states.

mine the conduction-band minimum to be at the X point, predicting that CaO is an indirect-band-gap material. However, no experimental study has so far shown that CaO has a minimum indirect band gap. Thus our results are consistent with the available experimental data in predicting the nature of the band gap for CaO.

No photoemission study in CaO is available with which we can compare the calculated valence-band width. We find the upper-valence-band width of 3.43 eV. The tight-binding and APW-LCAO calculations determine the width of 0.66 and 1.5 eV, respectively, whereas the tight-binding pseudopotential calculation finds a width of 8.36 eV.

In SrO, our calculations predict the uncorrelated band gap to be 14.85 eV, the long-range correction to be 2.85 eV, and the short-range correction to be 4.9 eV. The correlated band gap is then found to be 7.1 eV as compared to the experimental value of about 6.0 eV. (Table I).

We find both the valence-band maximum and the conduction-band minimum at the Γ point, predicting that SrO is a direct-band-gap material. Table V lists the energy gaps at high-symmetry points in SrO. The only other calculation based on the APW-LDA method²⁷ determines the conduction-band minimum at the X point, predicting that SrO is an indirect-band-gap material with the minimum direct band gap at the X point. As with the case of CaO, the available experimental studies have shown that SrO is a direct-band-gap material.

The density of states for SrO is given in Fig. 5. The width of the upper valence band is found to be 2.31 eV. We note here that the outermost p band of the Sr ion is placed in between the p and s bands of the oxygen ion.

The ϵ_2 spectrum of SrO shows two doublet structures with a separation of 0.23 eV. These structures have been assigned to the X and Γ excitations, respectively.² Assuming this assignment, one would then expect a different scenario for the band structure of SrO as compared to either MgO or CaO, such as a negligible dispersion of the top of the valence band and nearly the same positions for the Γ_{15} and X'_3 points in the conduction band. This is not what has been calculated with either Hartree-Fock or

TABLE IV. Prominent peak positions and their assignment in MgO. EPM is the empirical pseudo-potential method.

Peak position (eV)	This work	Pseudopotential-LDA ¹⁵	EPM (Ref. 21)
7.7	$\Gamma_{15}-\Gamma_1$	$\Gamma_{15}-\Gamma_1$	$\Gamma_{15}-\Gamma_1$
10.8	$L_3-L'_2$	X'_5-X_1	$L_3-L'_2$
13.3	X'_5-X_3	X'_5-X_3	$\Sigma_4-\Sigma_1$
16.8	X'_5-X_1	X'_4-X_3	X'_4-X_3

APW-LDA methods. We find a separation of 2.0 eV between the Γ and X energy gaps, whereas the APW-LDA calculation determines the separation to be 1.07 eV. Furthermore, the ϵ_2 spectrum of CaO and BaO shows only one doublet structure casting doubt on the assignment of the second doublet structure of SrO.

B. Alkaline-earth sulfides

The uncorrelated and correlated Hartree-Fock energy bands for alkaline-earth sulfides, namely MgS, CaS, and SrS are shown in Figs. 6–8. As is the case with oxides, the upper valence band is formed by the $3p$ orbitals of sulfur with a maximum at Γ . On the other hand, the minimum in the lower conduction band occurs at X for MgS and at Γ for CaS and SrS. Thus MgS is predicted to be an indirect-band-gap material while both CaS and SrS are predicted to be direct-band-gap materials.

Our calculation finds the uncorrelated direct band gap of 13.0, 12.2, and 11.6 eV for MgS, CaS, and SrS, respectively. The correlation corrections (on the order of 4.5 eV) reduce the gap to 8.4, 7.6, and 6.8 eV, for MgS, CaS,

and SrS, respectively. The corresponding estimated experimental values are about 5.6 and 5.0 eV for CaS and SrS, respectively (Table I). No experimental study is available for MgS. The energy gaps at high-symmetry points are given in Table VI along with the results of a linear augmented-plane-wave local-density-approximation (LAPW-LDA) calculation.²⁸ We note here that both calculations determine the top of valence band to be at Γ but differ considerably in predicting the conduction band.

The density of states for MgS and SrS is shown in Figs. 9 and 10, respectively. The upper-valence-band width comes out to be 8.56, 5.78, and 3.83 eV for MgS, CaS, and SrS, respectively. In CaS and SrS, the outermost p state of the cation does not lie inbetween the $3s$ and $3p$ states of the sulfur. This ordering of valence states is contrary to what we have observed for CaO and SrO.

In the ϵ_2 spectrum of CaS, two groups of peaks were observed with a separation of about 0.4 eV and were assigned to the excitons at X and Γ , respectively.² Our calculations, however, do not support this assignment and predict that the lowest exciton in these materials occur at

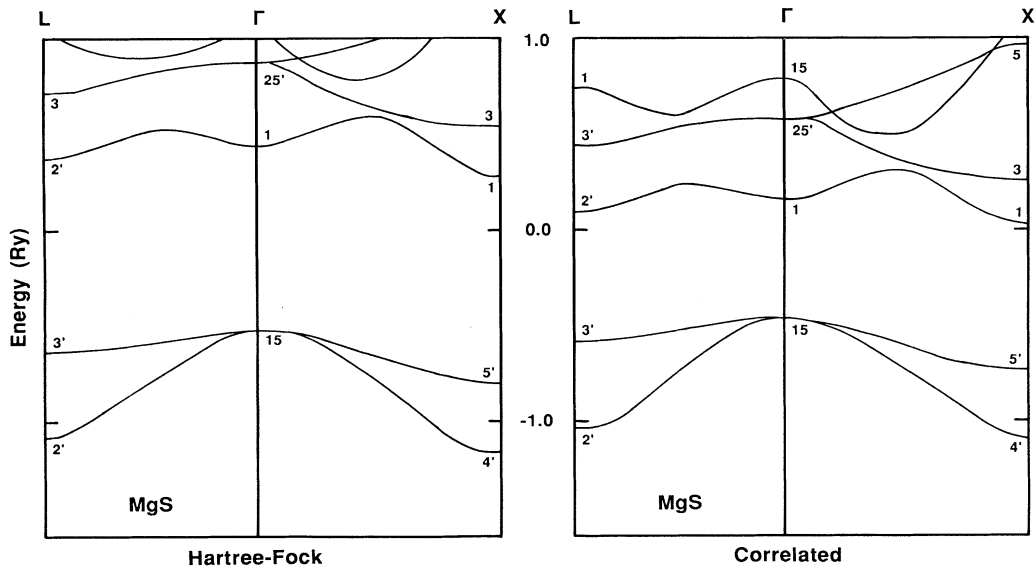


FIG. 6. MgS: Hartree-Fock and correlated energy bands.

TABLE V. Energy gaps (in eV) at high-symmetry points in CaO and SrO.

Method		Γ	Direct band gap		Indirect band gap
			X	L	
CaO	This work	7.74	11.99	14.13	10.81
	APW-LCAO ^a	9.71	9.74		9.62
	Tight-binding ^b	5.93	5.4		5.14
	Tight-binding-pseudopotential ^c	7.1	11.75	9.8	14.96
SrO	This work	7.11	9.11	12.36	8.54
	APW-LDA ^d	5.10	4.03	7.3	3.90

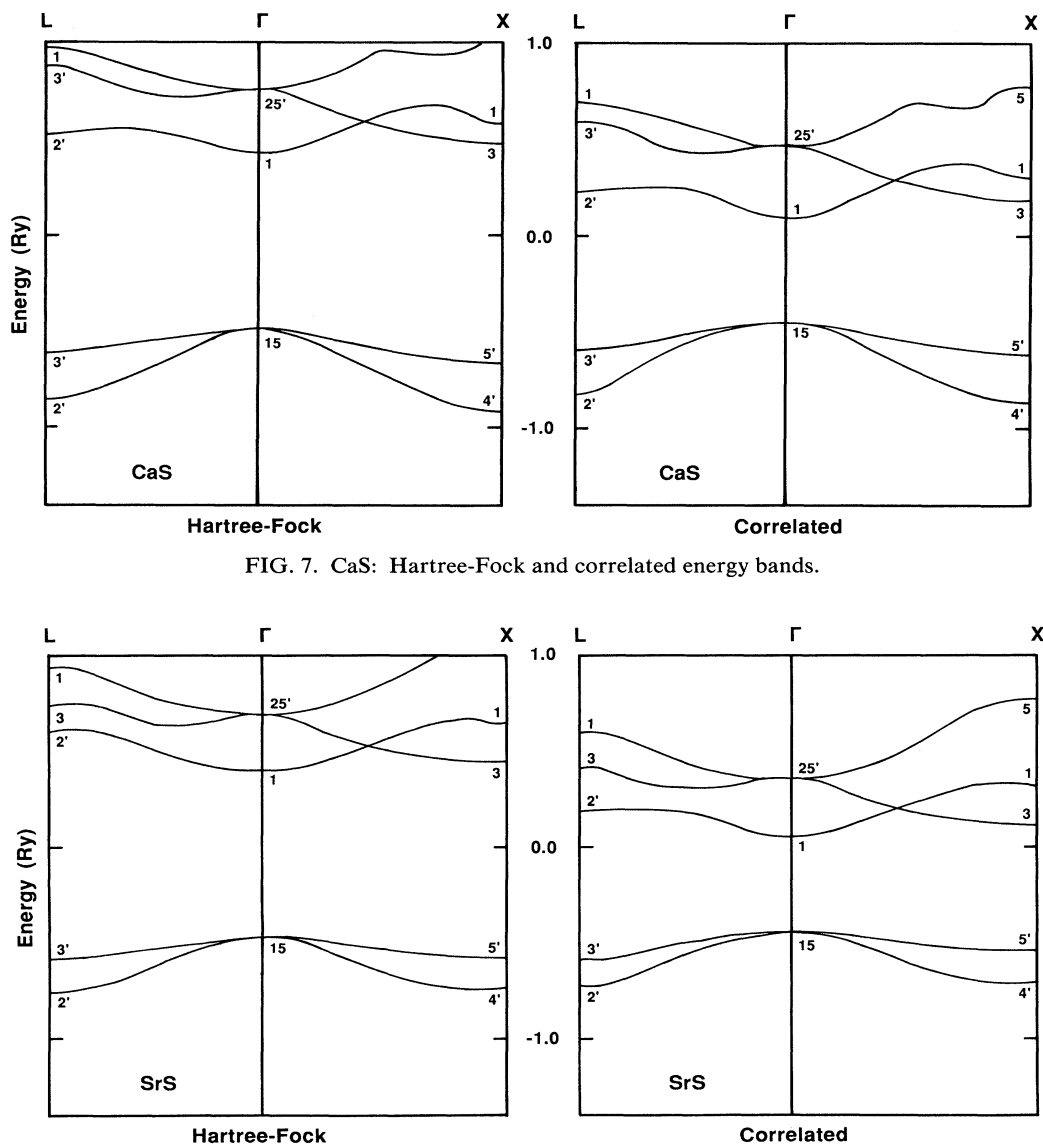
^aMattheiss, 1972 (Ref. 25).^bSeth and Chaney, 1975 (Ref. 26).^cDaud, Jouanin, and Gout, 1977 (Ref. 17).^dHasegawa and Yanase, 1980 (Ref. 27).

FIG. 7. CaS: Hartree-Fock and correlated energy bands.

FIG. 8. SrS: Hartree-Fock and correlated energy bands.

TABLE VI. Energy gaps (in eV) at high-symmetry points for sulfides.

		Energy gap				
		Direct band gap		Indirect band gap		
		Γ	X	L	$(\Gamma-X)$	$(\Gamma-L)$
MgS	This work	8.38	10.14	9.10	6.48	7.50
CaS	This work	7.60	12.64	10.97	10.39	9.43
	LAPW-LDA ^a	3.94	2.95	~5.5	2.14	3.16
SrS	This work	6.83	8.88	10.03	7.50	8.52
	LAPW-LDA ^a	3.51	2.78	~5.0	2.30	2.58

^aSelf-consistent linear augmented-plane-wave method with Kohn-Sham exchange potential (Ref. 28).

the Γ point. We note here that the LAPW-LDA calculation²⁸ assigns the first two peaks in the ϵ_2 spectrum to the transitions in the vicinity of Γ and L points with a separation of about 2.5 eV.

Sulfides are known to be highly reactive with oxygen. Furthermore, it has been shown that isoelectronic impurities can form an excitonic state near the band edge of the oxide.²⁹ We therefore suspect that the second peak in the ϵ_2 spectrum may be due to impurity excitonic states such as oxygen in sulfides.

IV. CONCLUSIONS

Alkaline-earth oxides and sulfides have the face-centered-cubic (rocksalt) structure. These materials are characterized by a high degree of ionicity (0.8–0.9) and can be considered as divalent cousins of alkali halides. The band structures of these materials can then be expected to exhibit the qualitative features shown by alkali halides. This is what we have found predicting that the lowest exciton occurs at the Γ point in these materials. Our results are therefore in disagreement with the results of the APW-LDA calculations which determine the lowest exciton at the X point in these materials.

Oxides are more ionic than sulfides and with this increased ionic character, oxides are expected to have a

larger gap than the corresponding sulfides as predicted in the present work. The calculated energies at the X point show the influence of the d -like branch, X'_3 in the conduction band. For MgO, the X_1 and X'_3 branches are nearly degenerate while in CaO and SrO the X'_3 branch is lower in the energy than the X_1 branch.

The degree of localization of the wave function at the ionic sites can also be seen from the calculated valence widths. The width decreases as we increase the nuclear charge of the cation, indicating that the wave function is more localized for SrX than for MgX (where X is O or S), consistent with the fact that SrX is more ionic than MgX.

In oxides, both the present work and the available experimental studies are in agreement in predicting the nature of the band gap. However, disagreement appears for sulfides. We believe that the only experimental study does not show with certainty that the band gap is indirect. For example, in SrS the fundamental absorption edge is reported to be about 5 eV. It was then argued that since the lower energy side of the absorption edge obeys the photon-energy dependence of the form of $(E - E_0)^3$, SrS is an indirect-band-gap material. However, as we have argued above, this absorption edge may well be in an impurity effect.

As for the overall magnitudes of the band gaps in these materials, we obtain the best agreement with experiment

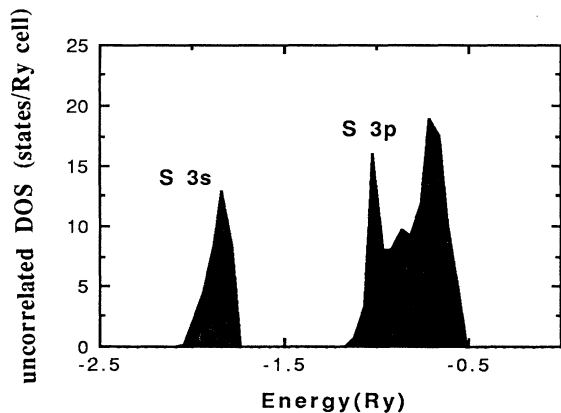


FIG. 9. MgS: density of states.

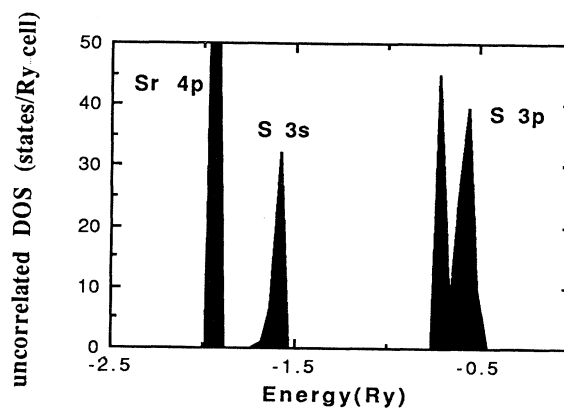


FIG. 10. SrS: density of states.

for the oxides, which is consistent with the fact that they are more ionic than the sulfides and hence can be more accurately treated by the local-orbitals form of Hartree-Fock theory than the more covalent sulfides. We also note that the local-density formalism is most accurate when treating a nearly uniform electron gas and hence may not be the best method for treating highly ionic materials where the charge density varies enormously from point to point.

Finally, we note here that extensive experimental information is lacking despite the fact that these materials are technologically important. We hope that this work will generate more interest among experimentalists.

ACKNOWLEDGMENTS

This work is supported by the U.S. Office of Naval Research under Contract No. ONR-N0014-89-J-160.

-
- ¹For a review, see R. Pandey and S. Sivaraman, *J. Phys. Chem. Solids* (to be published).
- ²(a) Y. Kaneko and T. Koda, *J. Cryst. Growth* **86**, 72 (1988); (b) Y. Kaneko, K. Morimoto, and T. Koda, *J. Phys. Soc. Jpn.* **52**, 4385 (1983).
- ³A. B. Kunz, *Phys. Rev. B* **26**, 2070 (1982).
- ⁴W. H. Adams, *J. Chem. Phys.* **37**, 2209 (1962); T. L. Gilbert, in *Molecular Orbitals in Chemistry, Physics, and Biology*, edited by P.-O. Löwdin and B. Pullman (Academic, New York, 1964), p. 405.
- ⁵A. B. Kunz, *Phys. Status Solidi* **36**, 301 (1969).
- ⁶S. T. Pantelides, D. J. Mickish, and A. B. Kunz, *Phys. Rev. B* **10**, 2602 (1974).
- ⁷A. B. Kunz, *Phys. Rev. B* **6**, 606 (1972), and references cited therein.
- ⁸A. B. Kunz and J. M. Vail, *Phys. Rev. B* **38**, 1058 (1988).
- ⁹D. M. Roessler and W. C. Walker, *Phys. Rev.* **159**, 733 (1967).
- ¹⁰R. C. Whited and W. C. Walker, *Phys. Rev.* **188**, 1380 (1969).
- ¹¹G. A. Saum and E. B. Hensley, *Phys. Rev.* **11**, 1019 (1959).
- ¹²R. C. Whited, C. J. Flaten, and W. C. Walker, *Solid State Commun.* **13**, 1903 (1973).
- ¹³V. S. Stepanyuk, A. Szasz, B. L. Grigorenko, O. V. Farberovich, and A. A. Katsnelson, *Phys. Status Solidi B* **155**, 179 (1989).
- ¹⁴Q. Weng and N. Holzwarth, *Phys. Rev. B* **41**, 5102 (1990).
- ¹⁵M. L. Bortz, R. G. French, D. J. Jones, R. V. Kasowski, and F. S. Ohuchi, *Phys. Scr.* **41**, 537 (1990).
- ¹⁶K. J. Chang and M. L. Cohen, *Phys. Rev. B* **30**, 4774 (1984).
- ¹⁷N. Daude, C. Jouanin, and C. Gout, *Phys. Rev. B* **15**, 2399 (1977).
- ¹⁸S. T. Pantelides, D. J. Mickish, and A. B. Kunz, *Phys. Rev. B* **10**, 5203 (1974).
- ¹⁹P. F. Walch and D. E. Ellis, *Phys. Rev. B* **8**, 5920 (1973).
- ²⁰J. Yamashita and S. Asano, *J. Phys. Soc. Jpn.* **28**, 1143 (1970).
- ²¹C. Y. Fong, W. Saslov, and M. L. Cohen, *Phys. Rev.* **168**, 992 (1968).
- ²²L. Fiermans, R. Hoogewijs, G. de Meyer, and J. Vennik, *Phys. Status Solidi A* **59**, 569 (1980).
- ²³W. F. Hanson, E. T. Arakawa, and M. W. Williams, *J. Appl. Phys.* **43**, 1661 (1972).
- ²⁴V. A. Fomichev, T. M. Zimkina, and III Zhukova, *Fiz. Tverd. Tela (Leningrad)* **10**, 3073 (1969) [*Sov. Phys.—Solid State* **10**, 2421 (1969)].
- ²⁵L. F. Mattheiss, *Phys. Rev. B* **5**, 290 (1972).
- ²⁶U. Seth and R. Chaney, *Phys. Rev. B* **12**, 5923 (1975).
- ²⁷A. Hasegawa and A. Yanase, *J. Phys. C* **13**, 1995 (1980).
- ²⁸V. S. Stepanyuk, A. Szasz, O. V. Farberovich, A. A. Grigorenko, A. V. Kozlov, and V. V. Mikhailin, *Phys. Status Solidi B* **155**, 215 (1989).
- ²⁹R. Pandey, J. Zuo, and A. B. Kunz, *Phys. Rev. B* **39**, 12 565 (1989).